Published in final edited form as:
Clin Cancer Res. 2016 July 1; 22(13): 3328–3339. doi:10.1158/1078-0432.CCR-15-1784.

STAT3/5-Dependent IL9 Overexpression Contributes to Neoplastic Cell Survival in Mycosis Fungoides

Pablo A. Vieyra-Garcia[1], **Tianling Wei**[2], **David Gram Naym**[2], **Simon Fredholm**[3], **Regina Fink-Puches**[1], **Lorenzo Cerroni**[1], **Niels Odum**[3], **John T. O'Malley**[4], **Robert Gniadecki**[2,5], and **Peter Wolf**[1]

[1]Research Unit for Photodermatology, Department of Dermatology and Venereology, Medical University of Graz, Graz, Austria

[2]Department of Dermatology, Bispebjerg Hospital, Copenhagen University Hospital, Copenhagen, Denmark

[3]Department of International Health, Immunology and Microbiology, University of Copenhagen, Copenhagen, Denmark

[4]Department of Dermatology, Brigham and Women's Hospital, Harvard University, Boston, Massachusetts

[5]Division of Dermatology, Department of Medicine, University of Alberta, Edmonton, Canada

Abstract

Purpose—Sustained inflammation is a key feature of mycosis fungoides (MF), the most common form of cutaneous T-cell lymphoma (CTCL). Resident IL9–producing T cells have been found in skin infections and certain inflammatory skin diseases, but their role in MF is currently unknown.

Experimental Design—We analyzed lesional skin from patients with MF for the expression of IL9 and its regulators. To determine which cells were producing IL9, high-throughput sequencing was used to identify malignant clones and Vb-specific antibodies were employed to visualize malignant cells in histologic preparations. To explore the mechanism of IL9 secretion, we knocked down STAT3/5 and IRF4 by siRNA transfection in CTCL cell lines receiving psoralen+UVA

Corresponding Author: Peter Wolf, Research Unit for Photodermatology, Department of Dermatology, Medical University of Graz, Auenbruggerplatz 8, Graz A-8036, Austria. Phone: 4331-6385-12371; Fax: 4331-6385-12466; peter.wolf@medunigraz.at.

Disclosure of Potential Conflicts of Interest
No potential conflicts of interest were disclosed.

Authors' Contributions
Conception and design: P.A. Vieyra-Garcia, R. Gniadecki, P. Wolf
Development of methodology: P.A. Vieyra-Garcia, T. Wei, J.T. O'Malley, P. Wolf
Acquisition of data (provided animals, acquired and managed patients, provided facilities, etc.): P.A. Vieyra-Garcia, T. Wei, D.G. Naym, S. Fredholm, R. Fink-Puches, L. Cerroni, N. Odum, R. Gniadecki, P. Wolf
Analysis and interpretation of data (e.g., statistical analysis, biostatistics, computational analysis): P.A. Vieyra-Garcia, T. Wei, S. Fredholm, L. Cerroni, N. Odum, R. Gniadecki, P. Wolf
Writing, review, and/or revision of the manuscript: P.A. Vieyra-Garcia, S. Fredholm, L. Cerroni, N. Odum, J.T. O'Malley, R. Gniadecki, P. Wolf
Administrative, technical, or material support (i.e., reporting or organizing data, constructing databases): P.A. Vieyra-Garcia, L. Cerroni, R. Gniadecki, P. Wolf
Study supervision: P. Wolf

Europe PMC Funders Author Manuscripts

(PUVA) ± anti-IL9 antibody. To further examine the role of IL9 in tumor development, the EL-4 T-cell lymphoma model was used in C57BL/6 mice.

Results—Malignant and reactive T cells produce IL9 in lesional skin. Expression of the Th9 transcription factor IRF4 in malignant cells was heterogeneous, whereas reactive T cells expressed it uniformly. PUVA or UVB phototherapy diminished the frequencies of IL9- and IL9r-positive cells, as well as STAT3/5a and IRF4 expression in lesional skin. IL9 production was regulated by STAT3/5 and silencing of STAT5 or blockade of IL9 with neutralizing antibodies potentiated cell death after PUVA treatment *in vitro*. IL9-depleted mice exhibited a reduction of tumor growth, higher frequencies of regulatory T cells, and activated CD4 and CD8 T lymphocytes.

Conclusion—Our results suggest that IL9 and its regulators are promising new targets for therapy development in mycosis fungoides.

Introduction

Mycosis fungoides (MF) is the most common type of cutaneous T-cell lymphoma (CTCL) accounting for about two thirds of all CTCLs and for almost half of all primary cutaneous lymphomas (1). MF is characterized by the expansion of malignant T cells in an environment of chronic inflammation primarily in the skin. Patients with MF usually present with fixed circumscribed patches and plaques that may persist for decades before progression to the tumor stage.

Malignant T cells in MF have a phenotype that resembles skin resident memory T (T_{RM}) cells by the expression of CD45RO (2), CCR4, CLA, and lack L-selectin (3). The vast majority of T cells in the skin are considered T_{RM}. In normal skin, T cells are found at a density of 10^6 cells/cm^2, making for a total of nearly 20 billion cells in the entire skin surface. This number accounts for almost twice the number of T cells in circulation (4). T_{RM} are a fundamental part of the skin immunity; however, their aberrant function results in chronic inflammatory diseases like psoriasis where they are able to initiate psoriatic lesions without T-cell recruitment from the blood in animal models (5).

MF lesions tend to relapse in the same location, another characteristic given by the possible T_{RM} origin of malignant cells. The presence of fixed lesions makes skin-directed therapies like topical retinoids or steroids and phototherapy with UVB or psoralen+UVA (PUVA) the first-line treatment options for patients with MF from stage I to IIA, according to EORTC-ISCL classification (1). Treatment with PUVA (6) or 311 nm narrowband UVB leads to complete remission in many patients with MF. Phototherapy has proapoptotic and immune-modulating properties (7), although the exact mechanisms by which this treatment leads to clearance of skin lesions of inflammatory skin conditions such as psoriasis and lymphoproliferative disorders like MF remain to be determined. For instance, in psoriasis, skin-infiltrating IL2r-bearing T-cell subsets were strongly suppressed after PUVA treatment, with almost complete elimination of these cells in some patients (8). Using the K5.hTGF-β1 mouse psoriasis model, we showed that PUVA induced clearance of skin lesions by downregulating the Th17/IL23 axis and simultaneous induction of regulatory T cells (Tregs; ref.9). This was consistent with the reduction of circulating Th17 cells and restoration of Tregs by photo(chemo)therapy observed in psoriasis patients. Nevertheless, Bath-PUVA

Europe PMC Funders Author Manuscripts

Europe PMC Funders Author Manuscripts

decreased the number of CCR4 tumor cells and Foxp3-positive cells in MF lesions, suggesting that treatment eliminates both malignant T cells and Tregs (10).

A large proportion of T_{RM} in the skin secretes IL9 with a distinctive Th9 phenotype (11). IL9 is a pleiotropic cytokine required for optimal secretion of effector cytokines and host defense in the skin against *C. albicans* (11), and in addition it potentiates angiogenesis and IL17 production in psoriasis (9). T lymphocytes secrete IL9 upon stimulation with IL2, IL4, and TGFβ by inhibition of BCL-6 (12), activation of IRF4 (13), and triggering of Smad2/3 (14), respectively. Though the *Il9* locus is responsive to several transcription factors, PU.1 (15) and IRF4 (13) have been proposed as master regulators of Th9 cells. We have shown that IRF4 is induced by STAT3 and STAT5 in T-cell lymphomas expressing nucleophosmin/anaplastic lymphoma kinase chimeric protein NPM/ALK, enhancing cell proliferation and protection from apoptosis (16). A growing body of evidence highlights the critical role of cytokine signaling in CTCL for survival and proliferation. IL13 acts as an autocrine factor that together with IL4 increases proliferation of malignant cells (17) and contributes to susceptibility of patients with MF to bacterial skin infections (18). IL21 stimulates activation of STAT3 in a positive regulatory loop in CTCL cell lines. However, its inhibition is insufficient to induce apoptosis or cell-cycle inhibition (19). IL32 is another cytokine upregulated in CTCL that potentiates cell survival and correlates with CCL17 and CCL18 expression (20). Herein, we report on the abundance of IL9 in MF lesions secreted by malignant and reactive T cells. Overexpression of STAT3/5 in malignant T cells drove IL9 secretion, suggesting an autocrine regulatory mechanism. IL9-producing cells had heterogeneous expression of IRF4 and no apparent dependence from PU.1. After photo(chemo)therapy, the number and relative frequency of IL9-positive cells was reduced as well as expression of IL9r, STAT3, and IRF4. We also provide evidence for the requirement of IL9 in tumor growth and its modulation of antitumor immune response in a mouse lymphoma model. Together, this points toward the crucial role of IL9 in the pathophysiology of MF at early stages.

Materials and Methods

Patients and human tissue samples

Human tissue samples were available from two sets of patients. By computer-assisted search in the electronic patient documentation system of the Phototherapy Unit (Department of Dermatology, Medical University of Graz, Graz, Austria) we identified archived, paraffin-embedded samples from eight patients with MF who had exhibited complete clinical and histologic response to photo(chemo)therapy. The patients had been treated with PUVA (n = 5) or 311-nm UVB (n = 3). The biopsies were taken before and after photo(chemo)therapy in the period from 2002 to 2012. The second set of tissue samples came from the patients of a clinical PUVA study (NCT01686594), where MF patients of clinical stage IA–IIB were treated in a standardized manner by oral PUVA (8-MOP, 10 mg per 20 kg of body weight; UVA twice a week). Biopsies were taken at baseline and after 6 weeks of therapy for further analysis. The characteristics of patients with MF are shown in Supplementary Table S2 and S3, respectively. Normal lesion-adjacent skin samples were available from patients undergoing surgery for skin lesions (i.e., melanocytic nevus or basal cell carcinoma). All

Europe PMC Funders Author Manuscripts

study procedures were approved by the ethics committee of the Medical University of Graz (Graz, Austria; protocols no. 25-294 ex 12/13; 24-169 ex 11/12; 21-080 ex 09/10; and 18-068 ex 06/07) and in compliance with the Declaration of Helsinki.

Cell lines

MyLa2000 and PB2B cells, derived from MF patients (21) and Hut78 derived from the blood of a patient with Sézary syndrome (22) were used for cell culture investigations. Hut78 cells were maintained in RPMI1640 medium with 10% FBS, 2 mmol/L L-glutamine, 1mmol/L sodium pyruvate, 10mmol/L HEPES, penicillin/streptomycin (50U/50 μg/mL). For the allograft lymphoma model, the mouse T-cell lymphoma cell line EL-4 was purchased from ATCC. MyLa2000 and EL-4 cells were maintained in high-glucose DMEM medium with 10% FBS, 50 mmol/L 2-mercaptoethanol and penicillin/streptomycin (50U/50 μg/mL).

RNA isolation and quantitative PCR

Total DNA and RNA were isolated from frozen tissue using the AllPrep DNA/RNA Mini Kit (Qiagen 80204) according to manufacturer's instructions. For cDNA synthesis, RNA (0.5 μg) was used for reverse transcription (Applied Biosystems, 4368814). cDNA (5 ng) was used to quantify expression of IL9, IRF4, and STAT3 (primer-list in ST1) by qPCR with Power SYBR Green (Applied Biosystems, 4367659). Samples were normalized to GAPDH and relative expression was calculated by the ΔC_t method.

For *in vitro* experiments, gene expression was quantified by purifying total RNA with RNeasy Mini Kit (Qiagen, 74104). cDNA was transcribed from 1 μg of RNA (Applied Biosystems, 4368814). qPCR was performed using TaqMan gene expression for IL9 and IL32 (Applied Biosystems, HS00914237-m1/HS00992441-m1). Gene expression was normalized on the basis of expression of reference gene GAPDH (Applied Biosystems, HS02758991-g1) and reported as relative units.

High-throughput sequencing analyses

DNA obtained from lesional MF skin was used to amplify the CDR3 regions of the TCR-β-chain for sequencing analysis by ImmunoSEQ (Adaptive Biotechnologies) from a 400 ng DNA template. A set of forward primers each specific to a functional TCR-βV segment and reverse primers to a specific to a TCR-βJ segment were used to amplify rearranged V(D)J segments for high-throughput sequencing at approximately 20× coverage. A clustering algorithm corrected sequencing errors and CDR3 segments were annotated, according to the international ImmunoGeneTics collaboration to enlist the contributing V, D, and J segments to every rearranged functional TCR (23). The distinct TCR were plotted on the basis of their frequency of appearance in the repertoire and ordered by the combination of TCR-βJ and TCR-βV genes in a 3D histogram. The putative malignant clone was identified by the abundance of sequence within the TCR repertoire.

Immunohistochemistry (IHC)

Paraffin-embedded skin sections were rehydrated in xylene and increasing dilutions of ethanol. Antigen retrieval was done using TRIS-EDTA pH9 buffer (Dako, S2367). The following antibodies were used: IL9 (Abcam, ab134434), IL9r (Abcam, ab61196), IRF4

(Abcam, ab124691), STAT3 (Abcam, ab50761-100), CD3 (Novocastra, NCL-CD3-PS1) and PU.1 (Abcam, ab76543). For single stains, the Peroxidase/AEC, rabbit/mouse REAL detection system (Dako, K5003) was used, as briefly described. After overnight incubation of the primary antibody, the slides were covered with a secondary antibody for 10 minutes, followed by streptavidin for 10 minutes, and finally the AEC/H_2O_2 substrate solution. Hematoxylin was used for nuclear counterstain. For cell quantification, the 40× objective was used and the area of the viewfield was calculated. Positive cells were counted in three different viewfields, and the mean values are presented.

Double stains were done using the MultiVision polymer detection system (Thermo Scientific, TL-012-MARH). After incubation with the primary antibody, the Ultra V block solution was applied for 10 minutes followed by the MultiVision polymer cocktail (anti-rabbit/HRP and anti mouse/AP) for 30 minutes. LVBlue chromogen (reacting with anti-mouse/AP immunoglobulins) was added for 10 minutes, followed by the LVRed chromogen (reacting with anti-rabbit/HRP immunoglobulins) for 10 minutes. Four washes with TBS-Tween 20 (0.5%) were done in between every step. For visualization of the malignant clone, we used the TCR sequencing data to select the anti-TCRVβ22 anti-body (Beckman Coulter, IM1484) to costain with IL9 and IRF4 the double stain system.

Selective inhibition of STAT and IRF4 by siRNA and JAK inhibition

Cells were transfected using the SMARTpool ON-TARGETplus–specific siRNA to STAT3, STAT5ab, or negative control siRNA (siCTRL; Thermo Scientific, L-003544-00-0005, L-005169-00-000, and L-010539-00-0005; 0.041 nmol/10^6 cells), siRNA targeting IRF4 (Ambion, AM16708-145051), or siCTRL (Ambion, AM4611; 0.05 nmol/10^6 cells) with an Amaxa Nucleofector protocol (Lonza). To confirm silencing, cells were lysed in RIPA buffer (EDTA 1%), protein quantification was done with Pierce BCA Protein Assay kit (Thermo Scientific), loaded in 4%–12% PAGE gels (Bio-Rad, 345-0125) and blotted on a 0.45-μm nitrocellulose membrane (Bio-Rad, 9004-70-0, 170-4071). Antibodies against IRF4 (Abcam, ab133590), STAT5, phospho-STAT5 (Y694), (Cell Signaling Technology; 9363 and 9356) or β-actin (Sigma, A5441) were used for Western blot analyses. MyLa2000 cells were treated with 180 μmol/L of ruxolitinib (Selleck Chemicals, INCB018424) and cultured to analyze IL9 expression by qPCR with the TaqMan method.

8-Methoxypsoralen and UVA irradiation *in vitro*

Cells were treated with 1 μmol/L of 8-Methoxypsoralen (8-MOP) 2 hours prior to UVA irradiation, a sublethal dose of UVA light (0.4 or 0.8 J/cm^2) was given and the cells were incubated in DMEM supplemented with 1,500 U/mL of IFNα2b (Merck-Millipore, GF417), 20 μg/mL of goat polyclonal anti-human IL9 antibodies (R&D Systems, AB-209-NA). For siRNA experiments, MyLa2000 cells were transfected with STAT5ab-siRNA or siCTRL and incubated for 24 hours prior to PUVA *in vitro*. Forty-eight hours after UVA irradiation, cells were double stained with the apoptosis kit Annexin V-FITC and PI (Beckman Coulter, PN-IM2375) and analyzed by flow cytometry (Beckman Coulter, Cell-Lab-Quanta-SC-MPL).

Europe PMC Funders Author Manuscripts

Intracellular staining and flow cytometry analyses

For experiments with Myla2000 and Hut78 cell lines, cells (0.5×10^6) were fixed and permeabilized with Fixation/Permeabilization buffer (eBioscience, 00-5123) for 30 minutes, followed by the staining with an isotype control antibody or an anti-IRF4-eFlour660 (eBioscience, 50-9858-82) in a permeabilization buffer (eBioscience, 00-8333) for 30 minutes.

For experiments with mice, cell suspensions were made by mincing lymph nodes in PBS. Cells (0.5×10^6) were stained with an anti-CD3-BrilliantViolet421 (Biolegend, 100335), anti-CD4-PercP (eBioscience, 45-0042-82), anti-CD8-APC (Biolegend, 100711), anti-CD44-PE-eFlour610 (eBioscience, 61-0441), and anti-CD62L-APC-Cy7 (Biolegend, 104428) for 20 minutes and acquired in the FACS LSR-II (BD Biosciences) and analyzed with FlowJo V9.3.2 (Tree Star).

IL9 ELISA

Production of IL9 was quantified in the supernatant of MyLa2000 and Hut78 cells using the Human IL9 ELISA kit (eBioscience, 88-7958-22). The assay was done according to the manufacturer's instructions with 50 μL of supernatant and the optical density was measured at 450 nm with a standard curve range of 1 to 100 pg/mL.

Tumor experiments in mice

Six-week-old C57BL/6 mice were shaved on the back with electric clippers and injected intradermally with 100 μL of EL4 cells (10^4 cells per mouse) to induce tumors. The animals were injected with 20 μg of goat isotype control (R&D Systems, ab-108-c) or blocking anti-IL9 (R&D Systems, ab-409-na) simultaneously with the EL-4 cells. Subsequently intralesional injections with the anti-IL9 or isotype control antibody were done every 48 hours. Tumor growth was assessed daily (on week days) by measuring two-diameter axes to calculate individual average (Mitutoyo, Mini-caliper). The animals were euthanized by cervical dislocation when tumor size reached 1 cm of diameter; skin samples and lymph nodes were taken for further analyses. Mice were held in a pathogen-free barrier facility. Animal work was done in accordance with our institutional guidelines on animal welfare with the approval by the Federal Ministry of Science, Research and Economy of Austria (BMWF-66.010/0022-II/3b/2013).

Statistical analysis

Data were analyzed for normal distribution with Shapiro test on SPSS 22 (IBM) and plotted with GraphPad Prism 6 (GraphPad). The statistical test chosen for each experiment is indicated in the figure legend.

Results

IL9 is abundantly produced by neoplastic and reactive T cells in MF lesional skin of patients with MF

Previous findings indicated the of IL9-producing skin-resident T cells in healthy individuals and inflammatory skin diseases such as psoriasis (9) and atopic dermatitis (24). We

examined skin biopsies from patients with MF and skin samples from healthy individuals by IHC. Normal skin had few IL9-producing cells (Fig. 1A), whereas a high number of IL9-positive cells were found in the dermis and dermoepidermal junction in MF skin lesions (Fig. 1B). Furthermore, we analyzed whether IL9 receptor (IL9r) and STAT3 were expressed in lesional MF skin. IL9r-positive cells were frequently present in lesional MF skin (Fig. 1B). We also observed positive nuclear stain of STAT3 in cells infiltrating the dermis. Normal skin stained negative for IL9r and only few cells were positive for STAT3 in the epidermis (Fig. 1A).

The fact that IL9-positive cells were located in the dermis and dermoepidermal junctions, particularly within Pautrier microabscesses (Fig. 1B) suggested that malignant T cells were indeed IL9 producers. To gain further insight about the IL9 source, we prepared immunohistochemical double stains of CD3/IL9 and STAT3/IL9 of lesional skin (Fig. 2A and B). The majority of IL9-positive cells were also CD3 positive and IL9 cells costained with STAT3.

Malignant clone identification in histologic sections relies mainly on cellular morphology, a caveat in distinguishing these cells from reactive T cells in lesional skin. We used high-throughput TCR-β CDR3 sequencing on DNA obtained from lesional skin to identify malignant clones. Results of a representative MF patient in tumor stage are shown in Fig. 2C. We observed an expanded number of sequence reads (blue bar indicative of an expanded malignant clone). This clone accounted for approximately 3% from all cells with functional (i.e., nonfragmented) T-cell receptors and had almost 10-fold higher frequency compared with the second most frequent clone (Supplementary Fig. S1A). The malignant clone carried the TCRβV02-01*01 and TCRβJ01-01*01 gene fragments identifiable by a commercially available Vb22 antibody (two different nomenclatures for TCR genes are used but TCRβV02-01 corresponds to Vb22). On the basis of the sequencing data, we estimated that approximately 38% from all Vb22-positive cells belonged to the malignant clone (Supplementary Fig. S1A). We found Vb22/IL9 double positive cells present at the basal epidermis and across the infiltrate of the dermis (Fig. 2D). We also found some IL9-producing cells negative for Vb22 suggesting an additional contribution of reactive T cells to the IL9-enriched microenvironment. To ensure the specificity of our stains, we used the combination of Vb22/isotype control antibody and Vb3/IL9. Vb22/isotype control antibody was negative while only a few Vb3 single positive cells and no Vb3/IL9 double positive cells were observed (Supplementary Fig. S1B). Taken together, these results indicate that neoplastic MF cells and reactive T cells overproduce IL9 compared with normal skin.

IL9 production in MF cell line MyLa2000 depends on JAK-STAT3/5 signaling

To further explore the mechanism of IL9 production in neoplastic MF T cells, we assessed whether IL9 production is maintained in CTCL cell lines. MyLa2000 and Hut78 cells were cultivated for 48 hours to determine IL9 production by qPCR and ELISA (Supplementary Fig. S2A). Whereas MyLa2000 cells highly expressed IL9 both at mRNA and protein level, we were unable to detect IL9 in Hut78 cells. Given that MyLa2000 cells have been used as an *in vitro* model for MF and its high production of IL9, we examined the role of JAK/STAT signaling in IL9 production by treating MyLa2000 cells with a selective JAK1/2 inhibitor

ruxolitinib. Treated cells showed a reduction of IL9 expression at 24 and 48 hours (Fig. 3A) without a significant loss of cell viability (Supplementary Fig. S2B). We transfected MyLa2000 cells with siRNAs targeting STAT3 or STAT5 and confirmed inhibition by Western blotting at 24 and 48 hours after transfection (Supplementary Fig. S3A). siSTAT5-transfected cells had a high reduction of IL9 expression at 24 hours. By 48 hours, both siSTAT3 and siSTAT5 reduced significantly IL9 expression (Fig. 3B and C). To confirm these observations, we quantified IL9 by ELISA in the supernatant of MyLa2000 cells after individual or simultaneous siSTAT3 and siSTAT5 transfection. Consistent with the mRNA results, siSTAT5 was more efficient at reducing IL9 secretion (Fig. 3D). However, we did not observe an additive effect of simultaneous transfection at 48 hours, although by 72 hours, the reduction of IL9 was higher in simultaneously silenced cells compared with their individually transfected counterparts (Fig. 3D). Expression of IL32 was measured as control of the specific effect of STAT3/5 siRNA transfection on IL9 secretion; MyLa2000 did not show a change in IL32 secretion for up to 48 hours of transfection (Fig. 3E). PB2B cells also exhibited spontaneous IL9 production that was downregulated by STAT3/5 siRNA transfection (Supplementary Fig. S4). These findings indicate that JAK signaling regulates IL9 production via STAT3/5-dependent mechanism.

Role of IRF4 and PU.1 transcription factors in MF

To address whether malignant cells expressed Th9-related transcription factors, we prepared double stains of CD3/IRF4 (Fig. 4A) and CD3/PU.1 (Fig. 4B) of lesional skin. CD3-positive cells costained with IRF4 while all PU.1-positive cells were CD3-negative (detailed information about double stains is shown in Supplementary Table S2). To further analyze expression of IRF4 in malignant T cells, we performed a double stain for Vb22/IRF4 (Fig. 4C). We observed that some Vb22-positive cells expressed IRF4; we also found IRF4 single positive cells with lymphocyte morphology (Fig. 4A) suggesting that IL9 expression in T cells is independent of PU.1 and that IRF4 is likely to be involved in both malignant and reactive T-cell IL9 production.

Following our observation of IRF4 expression in malignant and reactive T cells, we analyzed the role of this transcription factor *in vitro*. MyLa2000 cells expressed IRF4, whereas Hut78 cells lacked expression of this transcription factor (Fig. 4D). Flow cytometry analyses showed that MyLa2000 had a high expression of IRF4, whereas Hut78 cells displayed only a discrete expression (Supplementary Fig. S5A). Consistent with these results, siIRF4-transfected MyLa2000 cells showed a reduction of IL9 expression by 60% and 80% at 24 and 96 hours, respectively, after transfection (Fig. 4E). Although transfection efficacy of siIRF4 was only 20%, this was sufficient to observe an effect on IL9 expression and did not compromise cell viability compared with siCTRL (Supplementary Fig. S5B). In addition, Hut78 cells were mainly PU.1-negative while MyLa2000 cells had a low expression of PU.1 (Supplementary Fig. S3B). Together our data indicate that IRF4 is expressed in lesional skin of patients with MF and regulates IL9 production in neoplastic cells.

PUVA depletes IL9-producing cells in MF lesions

As IL9 is overexpressed in MF skin lesions, we wanted to examine whether clinical response to phototherapy correlates with a decrease in IL9-producing cells. Biopsies taken at baseline and after 6 to 45 weeks of treatment at complete clinical remission were available for further analysis (detailed information about the patients and their treatment can be found in Supplementary Table S2). As depicted in Fig. 1, we found a high number of IL9-positive cells infiltrating the dermis prior to therapy. After phototherapy treatment, the total infiltrate of IL9-positivecells was reduced by 69% (from 245 to 77 cells/mm^2; Fig. 5A). In addition, we stained for IL9r to assess the potential number of cells responsive to IL9 before and after treatment. We observed a substantial reduction of IL9r-positive cells by 64% (from 187 cells/mm^2 before treatment to 68 cells/mm^2 after treatment; Fig. 5B).

Furthermore, we analyzed fresh material from patients receiving oral PUVA with 8-MOP twice a week in a clinical study (detailed information about the patients and their treatment can be found in Supplementary Table S3). Biopsies taken at baseline (before treatment) and after 6 weeks of treatment were available to evaluate response. We found that IL9 and STAT3 expression was decreased in lesional skin after treatment in 6 of 8 patients (Fig. 5C and D). IRF4 (Supplementary Fig. S5C) and STAT5a (Supplementary Fig. S6A) were also decreased in patients after treatment while STAT5b did not change significantly (Supplementary Fig. S2B). Furthermore, analyses of infiltration degree coupled with STAT3 or IRF4 expression revealed a correlation between high expression of these transcription factors and higher cellular infiltration of the skin (Supplementary Fig. S6A and S6D). These results indicate that photo(chemo)therapy in patients with MF depletes IL9 in lesional skin together with lowering expression of elements of the JAK/STAT signaling pathway.

Proapoptotic effect of PUVA is enhanced by IL9 depletion *in vitro*

The combination of PUVA and IFNα2b at variable doses increases the efficacy of phototherapy in MF patients; decreasing the number of PUVA sessions and the dose of UVA needed to achieve remission (25). To address how the effect of PUVA combined with IL9 targeting or STAT5 inhibition compares with supplementation of IFNα2b, we transfected MyLa2000 cells with siRNA targeting STAT5 24 hours prior to PUVA *in vitro* (1 μmol/L 8-MOP, 0.4 J/cm^2 UVA). After 48 hours of PUVA, we observed a lower expression of IRF4 and IL9 and higher expression of pSTAT5 (Supplementary Fig. S7A–S7D). Moreover, cell viability decreased in PUVA/siSTAT5–treated cells to 18% compared with 8-MOP alone (58%) and PUVA/siCTRL (42%; Fig. 5E). We used an IL9-neutralizing antibody to evaluate the role of this cytokine in malignant cell viability after combining PUVA with IFNα2b. Cells were treated with PUVA and cultured for 48 hours with IFNα2b (1,500 U/mL), goat polyclonal anti-human IL9 (20 μg/mL) or the two combined. The combination of PUVA with IFN-α2b reduced cell viability to 38% compared with PUVA treatment alone (56%); PUVA/anti-IL9 treatment showed a reduction of viability to 37% and the combination of PUVA/IFNα2b/anti-IL9 reduced viability with small additive effect down to 35%. These data indicate that direct targeting of IL9 or its regulators potentiates PUVA's cytotoxicity against malignant lymphoma cells similar to the addition of IFNα2b (Fig. 5F).

Depletion of IL9 inhibits tumor growth and improves antitumor response in a lymphoma mouse model

Having established the high production of IL9 of malignant and reactive T cells in MF lesions and the dependence from STAT3/5 signaling *in vitro*, we aimed to investigate the functional significance of this cytokine in MF. We initially hypothesized that IL9 may affect growth of lymphoma cells. However, experiments with MyLa2000 cells did not reveal a significant effect of exogenous IL9 or IL9 antibody blockade on cell growth or apoptosis (data not shown). We subsequently considered that IL9 might modulate the growth of lymphoma cells in the tissue, rather than in cell suspension. Therefore, we evaluated tumor growth in a lymphoma mouse model. We injected intradermally C57BL/6 mice with the mouse T-cell lymphoma cell line EL-4 and blocked IL9 by intralesional injections of anti-IL9-neutralizing antibody every 48 hours (Fig. 6A). The tumor diameter growth curve showed slower tumor formation in the anti-IL9-treated animals (Fig. 6B) and survival was extended by 50% (from 16 to 24 days; Fig. 6C) compared with isotype antibody control group. To analyze the effect of anti-IL9 treatment on antitumor immune response, draining lymph nodes were collected at 14 days after lymphoma cell injections. Anti-IL9-treated mice had a higher percentage of $CD25^{+}Foxp3^{+}$ T cells compared with isotype-treated antibody control mice (14.5% vs. 11% respectively; Fig. 6D). Frequency of antigen-experienced ($CD44^{high}/CD62l^{low}$) CD4 and CD8 T cells were higher in anti-IL9-treated animals compared with isotype antibody-treated controls (10% and 8% vs. 5% and 3%, respectively; Fig. 6D). Together these results suggest that IL9 is required for tumor growth and modulates the antitumor immune response.

Discussion

This study revealed that lesional MF skin is enriched with cells producing IL9 expressing STAT3 and IL9r. STAT3 is an important member of the signaling pathway activated in IL9-producing cells. It is recruited upon IL9 binding to its receptor via its SH2 domain (26) and is crucial for apoptosis inhibition (27). More recently, its expression in Sézary syndrome cells has been attributed to a positive feedback loop of IL21 (19). In the patients of this study, IL9-producing cells were mainly located within the infiltrate in the dermis and in Pautrier's microabscesses (Fig. 1B), a site that primarily harbors malignant T cells. Furthermore, IL9-positive cells decreased in lesional skin after complete clinical response (Fig. 5A) in the set of patients from archived materials. These findings were consistent with the results of IL9 mRNA expression (Fig. 5C) in the set of patients from the clinical PUVA trial (Supplementary Table S3).

High-throughput TCR sequencing analysis allowed us to identify and subsequently visualize malignant T-cell clones *in situ*. We found that the vast majority of Vb22-expressing malignant clones were IL9 producers (Fig. 2C and D). However, we also observed IL9 production from presumably benign infiltrating T cells suggesting that IL9 production is not specific to the neoplastic population. We hypothesize that malignant clones produce significant amounts of IL9 that polarize the cytokine secretion of reactive T cells towards a Th9 profile. Consistently, many of these cells were IRF4-positive. Previous reports illustrated how malignant clones are able to decrease Th1 responses in favor to Th2 in

leukemic CTCL, in a similar manner (28). Moreover, deregulation of IL9 has been described for several types of lymphoma and can contribute not only to the replication of malignant cells (29) but also modulate the inflammatory microenvironment (30).

The constant activation of STAT family members has been implicated in the pathogenesis of a wide variety of lymphomas (29, 31) including CTCL. Gain of function in this family of proteins has been observed as a result of chromosome instability (32) or activating mutations in STAT3 p.Tyr640Phe (33) and STAT5 (34). We have shown that expression of JAK3 and two members of the STAT family in Sézary syndrome and MF cell lines leads to IL17 secretion (35). Studies *in vitro* with CTCL cell lines have revealed that the activated form of STAT3 leads to the expression of SOCS-3, a negative regulator of IFNα-induced signaling (36). Moreover, STAT3 is activated by IL9r together with STAT5 and in a lesser extent by STAT1 (37). Here we found that MyLa2000 cells produced high amounts of IL9 (S2) in accordance with our findings in MF lesional skin. Furthermore the combination of PUVA with IFNα and/or anti-IL9 antibody or silencing of STAT5 reduced cell viability (Fig. 5E and F), highlighting the possible mechanisms that mediate the conceivable better response of MF patients treated with PUVA in combination with biologic agents (38).

The inhibition of JAK1/2 with ruxolitinib led to a significant reduction of IL9 secretion (Fig. 3A), and the silencing of STAT3/5 (Fig. 3B–D) suggested a self-regulatory loop of IL9 production in MyLa2000 cells. BCL-6 is known as a negative regulator of IL9 transcription and is inhibited by STAT5 through binding to its regulatory region (39), STAT5 also activates IRF4 (40) and mediates directly the binding to the *Il9* gene (41). The multiple involvement of STAT5 in the regulation of IL9 may explain the profound impact of its silencing in our results although we only observed a significant reduction in STAT5a in the skin of PUVA-treated patients (Supplementary Fig. S6A).

We did not find CD3-positive cells with PU.1 expression in lesional skin of MF (Fig. 4B). The lack of its expression in MyLa2000 cells supports the notion that PU.1 does not mediate IL9 secretion in neoplastic MF T cells. However, we did find PU.1-positive cells in the proximity of T cells suggesting a close interaction between these two populations; further analysis revealed that PU.1 cells were CD1a-positive with dendritic cell like morphology (data not shown). Our argument on the role of IRF4 in IL9 secretion by malignant T cells is supported by the finding that even partial inhibition of IRF4 in MyLa2000 cells led to a significant decrease in IL9 production (Fig. 4D and E) and that PUVA-treated patients exhibited reduced IRF4 expression in lesional skin (Supplementary Fig. S5C). However, the precise role of IRF4 remains to be determined as Vb22-positive cells exhibited heterogeneous expression of this transcription factor (4 out of every 10 cells were IRF4-positive; Fig. 4C) while most (Vb22-negative) reactive T cells seemed to stain IRF4-positive (Fig. 4A).

We observed an overall decrease of infiltrate and IL9 microenvironment: Patients with complete response to photo(chemo) therapy had significantly lower numbers of IL9- and IL9r-positive cells in treated skin (Fig. 5A and B). PUVA-treated patients also showed a reduction of IL9 and STAT3 expression (Fig. 5C and D). Patients with high expression of IRF4 in lesional skin at baseline reduced the expression of this transcription factor after

Europe PMC Funders Author Manuscripts

treatment (Supplementary Fig. S5C) and a decrease of infiltration score correlated with lower STAT3 and IRF4 expression (Supplementary Fig. S6C and D).

Although there is one report on sporadic CTCL-like disease in mice (42), intradermal injection of murine lymphoma cell lines like MBL2 and EL-4 have been the best approximation of a CTCL model in mice (43, 44). In contrast to xenograft models, syngeneic engraftments take into account immunologic interactions between lymphoma cells and the host. EL-4 cells have been used in several lymphoma models of iNKT cytotoxic responses (45) and adipose tissue mesenchymal stem cells (46). We used these cells because tumors are developed without a proinflammatory external stimulus and their responsiveness to IL9 with expression of growth factors such as Ly-6A/E (47) and 24p3 lipocalin (48). Our results showed that EL-4 tumors grew significantly slower in IL9-depleted mice (Fig. 6B and C) while the percentage of activated CD4 and CD8 T cells increased substantially (Fig. 6E and F). However, we recognize the lack of epidermotropism (typically seen in MF) as the major limitation of our animal model. Another limitation of this report is that high-throughput TCR sequencing analysis was done in a single patient (Fig. 2). Nevertheless the results point towards the importance of IL9 as stimulatory mediator in MF.

Taken together, our results describe an IL9-enriched microenvironment in MF lesions by malignant and reactive T cells as the source of this cytokine. We found that STAT3/5 are coregulators of IL9 production *in vitro*. Furthermore, 16 patients with complete or partial response to photo(chemo)therapy exhibited decreased expression of IL9, STAT3, STAT5a, and IRF4. We also demonstrate the delayed development of lymphoma and improvement of antitumor T-cell response in the EL-4 syngeneic mouse skin lymphoma model. The evidence presented indicates that targeting IL9 or its mediators could be a promising new approach for the treatment of CTCL.

Supplementary Material

Refer to Web version on PubMed Central for supplementary material.

Acknowledgments

The authors thank the patients who donated skin samples that made this work possible. Gerlinde Mayer and Ulrike Schmidbauer are acknowledged for their help with histologic stains. Drs. Alexandra Gruber-Wackernagel, Angelika Hofer, and Franz J. Legat, Department of Dermatology, Medical University of Graz, administered phototherapy, and Dr. Michael Horn, Medical University of Graz, helped building-up a tissue bank of normal skin samples. The authors specially thank Dr. Rachael Clark from Harvard University (Boston, MA) for many helpful comments and suggestions as well as Dr. Honnavara N. Ananthaswamy The University of Texas, M.D. Anderson Cancer Center (Houston, Texas) for critical reading and editing of the manuscript.

Grant Support

This work was supported by the Oesterreichische Nationalbank Anniversary Fund project no.15463 and FWF-Austrian-Science-Fund no.W1241. P.A. Vieyra-Garcia was supported by the PhD program Molecular Fundamentals of Inflammation (MOLIN) from the Medical University of Graz, Austria and CONACYT-Mexico.

The costs of publication of this article were defrayed in part by the payment of page charges. This article must therefore be hereby marked *advertisement* in accordance with 18 U.S.C. Section 1734 solely to indicate this fact.

References

1. Olsen E, Vonderheid E, Pimpinelli N, Willemze R, Kim Y, Knobler R, et al. Revisions to the staging and classification of mycosis fungoides and Sezary syndrome: a proposal of the International Society for Cutaneous Lymphomas (ISCL) and the cutaneous lymphoma task force of the European Organization of Research and Treatment of Cancer (EORTC). Blood. 2007; 110:1713–22. [PubMed: 17540844]
2. Ismail SA, Han R, Sanborn SL, Stevens SR, Cooper KD, Wood GS, et al. Immunohistochemical staining for CD45R isoforms in paraffin sections to diagnose mycosis fungoides-type cutaneous T-cell lymphoma. J Am Acad Dermatol. 2007; 56:635–42. [PubMed: 17367612]
3. Campbell JJ, Clark RA, Watanabe R, Kupper TS. Sezary syndrome and mycosis fungoides arise from distinct T-cell subsets: a biologic rationale for their distinct clinical behaviors. Blood. 2010; 116:767–71. [PubMed: 20484084]
4. Clark RA, Chong B, Mirchandani N, Brinster NK, Yamanaka K, Dowgiert RK, et al. The vast majority of CLA+ T cells are resident in normal skin. J Immunol. 2006; 176:4431–9. [PubMed: 16547281]
5. Boyman O, Hefti HP, Conrad C, Nickoloff BJ, Suter M, Nestle FO. Spontaneous development of psoriasis in a new animal model shows an essential role for resident T cells and tumor necrosis factor-alpha. J Exp Med. 2004; 199:731–6. [PubMed: 14981113]
6. Whittaker S, Ortiz P, Dummer R, Ranki A, Hasan B, Meulemans B, et al. Efficacy and safety of bexarotene combined with psoralen-ultraviolet A (PUVA) compared with PUVA treatment alone in stage IB-IIA mycosis fungoides: final results from the EORTC Cutaneous Lymphoma Task Force phase III randomized clinical trial (NCT00056056). Br J Dermatol. 2012; 167:678–87. [PubMed: 22924950]
7. Wolf P, Nghiem DX, Walterscheid JP, Byrne S, Matsumura Y, Matsumura Y, et al. Platelet-activating factor is crucial in psoralen and ultraviolet A-induced immune suppression, inflammation, and apoptosis. Am J Pathol. 2006; 169:795–805. [PubMed: 16936256]
8. Vallat VP, Gilleaudeau P, Battat L, Wolfe J, Nabeya R, Heftler N, et al. PUVA bath therapy strongly suppresses immunological and epidermal activation in psoriasis: a possible cellular basis for remittive therapy. J Exp Med. 1994; 180:283–96. [PubMed: 7516410]
9. Singh TP, Schon MP, Wallbrecht K, Gruber-Wackernagel A, Wang XJ, Wolf P. Involvement of IL-9 in Th17-associated inflammation and angiogenesis of psoriasis. PloS One. 2013; 8:e51752. [PubMed: 23335955]
10. Kato H, Saito C, Ito E, Furuhashi T, Nishida E, Ishida T, et al. Bath-PUVA therapy decreases infiltrating CCR4-expressing tumor cells and regulatory T cells in patients with mycosis Fungoides. Clin Lymphoma Myeloma Leuk. 2013; 13:273–80. [PubMed: 23332394]
11. Schlapbach C, Gehad A, Yang C, Watanabe R, Guenova E, Teague JE, et al. Human TH9 cells are skin-tropic and have autocrine and paracrine proinflammatory capacity. Sci Transl Med. 2014; 6:219ra8.
12. Bassil R, Orent W, Olah M, Kurdi AT, Frangieh M, Buttrick T, et al. BCL6 controls Th9 cell development by repressing Il9 transcription. J Immunol. 2014; 193:198–207. [PubMed: 24879792]
13. Staudt V, Bothur E, Klein M, Lingnau K, Reuter S, Grebe N, et al. Interferon-regulatory factor 4 is essential for the developmental program of T helper 9 cells. Immunity. 2010; 33:192–202. [PubMed: 20674401]
14. Tamiya T, Ichiyama K, Kotani H, Fukaya T, Sekiya T, Shichita T, et al. Smad2/3 and IRF4 play a cooperative role in IL-9-producing T cell induction. J Immunol. 2013; 191:2360–71. [PubMed: 23913959]
15. Chang HC, Sehra S, Goswami R, Yao W, Yu Q, Stritesky GL, et al. The transcription factor PU.1 is required for the development of IL-9-producing T cells and allergic inflammation. Nat Immunol. 2010; 11:527–34. [PubMed: 20431622]
16. Marzec M, Halasa K, Liu X, Wang HY, Cheng M, Baldwin D, et al. Malignant transformation of CD4+ T lymphocytes mediated by oncogenic kinase NPM/ALK recapitulates IL-2-induced cell signaling and gene expression reprogramming. J Immunol. 2013; 191:6200–7. [PubMed: 24218456]

Europe PMC Funders Author Manuscripts

17. Geskin LJ, Viragova S, Stolz DB, Fuschiotti P. Interleukin-13 is overexpressed in cutaneous T-cell lymphoma cells and regulates their proliferation. Blood. 2015; 125:2798–805. [PubMed: 25628470]
18. Wolk K, Mitsui H, Witte K, Gellrich S, Gulati N, Humme D, et al. Deficient cutaneous antibacterial competence in cutaneous T-cell lymphomas: role of Th2-mediated biased Th17 function. Clin Cancer Res. 2014; 20:5507–16. [PubMed: 25212608]
19. van der Fits L, Out-Luiting JJ, Tensen CP, Zoutman WH, Vermeer MH. Exploring the IL-21-STAT3 axis as therapeutic target for Sezary syndrome. J Invest Dermatol. 2014; 134:2639–47. [PubMed: 24756111]
20. Suga H, Sugaya M, Miyagaki T, Kawaguchi M, Fujita H, Asano Y, et al. The role of IL-32 in cutaneous T-cell lymphoma. J Invest Dermatol. 2014; 134:1428–35. [PubMed: 24226419]
21. Kaltoft K, Bisballe S, Dyrberg T, Boel E, Rasmussen PB, Thestrup-Pedersen K. Establishment of two continuous T-cell strains from a single plaque of a patient with mycosis fungoides. In Vitro Cell Dev Biol. 1992; 28A:161–7. [PubMed: 1582990]
22. Poiesz BJ, Ruscetti FW, Mier JW, Woods AM, Gallo RC. T-cell lines established from human T-lymphocytic neoplasias by direct response to T-cell growth factor. Proc Natl Acad Sci U S A. 1980; 77:6815–9. [PubMed: 6256763]
23. Lefranc MP. IMGT, the International ImMunoGeneTics Information System. Cold Spring Harbor Protocols. 2011; 2011:595–603. [PubMed: 21632786]
24. Ma L, Xue HB, Guan XH, Shu CM, Zhang JH, Yu J. Possible pathogenic role of T helper type 9 cells and interleukin (IL)-9 in atopic dermatitis. Clin Exp Immunol. 2014; 175:25–31. [PubMed: 24032555]
25. Nikolaou V, Siakantaris MP, Vassilakopoulos TP, Papadavid E, Stratigos A, Economidi A, et al. PUVA plus interferon alpha2b in the treatment of advanced or refractory to PUVA early stage mycosis fungoides: a case series. J Eur Acad Dermatol Venereol. 2011; 25:354–7. [PubMed: 20586838]
26. Lejeune D, Demoulin JB, Renauld JC. Interleukin 9 induces expression of three cytokine signal inhibitors: cytokine-inducible SH2-containing protein, suppressor of cytokine signalling (SOCS)-2 and SOCS-3, but only SOCS-3 overexpression suppresses interleukin 9 signalling. Biochem J. 2001; 353:109–16. [PubMed: 11115404]
27. Demoulin JB, Van Roost E, Stevens M, Groner B, Renauld JC. Distinct roles for STAT1, STAT3, and STAT5 in differentiation gene induction and apoptosis inhibition by interleukin-9. J Biol Chem. 1999; 274:25855–61. [PubMed: 10464327]
28. Guenova E, Watanabe R, Teague JE, Desimone JA, Jiang Y, Dowlatshahi M, et al. TH2 cytokines from malignant cells suppress TH1 responses and enforce a global TH2 bias in leukemic cutaneous T-cell lymphoma. Clin Cancer Res. 2013; 19:3755–63. [PubMed: 23785046]
29. Chen N, Lu K, Li P, Lv X, Wang X. Overexpression of IL-9 induced by STAT6 activation promotes the pathogenesis of chronic lymphocytic leukemia. Int J Clin Exp Pathol. 2014; 7:2319–23. [PubMed: 24966942]
30. Lange K, Uckert W, Blankenstein T, Nadrowitz R, Bittner C, Renauld JC, et al. Overexpression of NPM-ALK induces different types of malignant lymphomas in IL-9 transgenic mice. Oncogene. 2003; 22:517–27. [PubMed: 12555065]
31. Sommer VH, Clemmensen OJ, Nielsen O, Wasik M, Lovato P, Brender C, et al. In vivo activation of STAT3 in cutaneous T-cell lymphoma. Evidence for an antiapoptotic function of STAT3. Leukemia. 2004; 18:1288–95. [PubMed: 15141228]
32. Wang L, Ni X, Covington KR, Yang BY, Shiu J, Zhang X, et al. Genomic profiling of Sezary syndrome identifies alterations of key T cell signaling and differentiation genes. Nat Genet. 2015; 47:1426–34. [PubMed: 26551670]
33. da Silva Almeida AC, Abate F, Khiabanian H, Martinez-Escala E, Guitart J, Tensen CP, et al. The mutational landscape of cutaneous T cell lymphoma and Sezary syndrome. Nat Genet. 2015; 47:1465–70. [PubMed: 26551667]
34. Choi J, Goh G, Walradt T, Hong BS, Bunick CG, Chen K, et al. Genomic landscape of cutaneous T cell lymphoma. Nat Genet. 2015; 47:1011–9. [PubMed: 26192916]

35. Krejsgaard T, Ralfkiaer U, Clasen-Linde E, Eriksen KW, Kopp KL, Bonefeld CM, et al. Malignant cutaneous T-cell lymphoma cells express IL-17 utilizing the Jak3/Stat3 signaling pathway. J Invest Dermatol. 2011; 131:1331–8. [PubMed: 21346774]
36. Brender C, Nielsen M, Kaltoft K, Mikkelsen G, Zhang Q, Wasik M, et al. STAT3-mediated constitutive expression of SOCS-3 in cutaneous T-cell lymphoma. Blood. 2001; 97:1056–62. [PubMed: 11159537]
37. Shang Y, Kakinuma S, Amasaki Y, Nishimura M, Kobayashi Y, Shimada Y. Aberrant activation of interleukin-9 receptor and downstream Stat3/5 in primary T-cell lymphomas in vivo in susceptible B6 and resistant C3H mice. In Vivo. 2008; 22:713–20. [PubMed: 19180996]
38. Chiarion-Sileni V, Bononi A, Fornasa CV, Soraru M, Alaibac M, Ferrazzi E, et al. Phase II trial of interferon-alpha-2a plus psolaren with ultraviolet light A in patients with cutaneous T-cell lymphoma. Cancer. 2002; 95:569–75. [PubMed: 12209749]
39. Walker SR, Nelson EA, Frank DA. STAT5 represses BCL6 expression by binding to a regulatory region frequently mutated in lymphomas. Oncogene. 2007; 26:224–33. [PubMed: 16819511]
40. Laurence A, Tato CM, Davidson TS, Kanno Y, Chen Z, Yao Z, et al. Interleukin-2 signaling via STAT5 constrains T helper 17 cell generation. Immunity. 2007; 26:371–81. [PubMed: 17363300]
41. Yao W, Zhang Y, Jabeen R, Nguyen ET, Wilkes DS, Tepper RS, et al. Interleukin-9 is required for allergic airway inflammation mediated by the cytokine TSLP. Immunity. 2013; 38:360–72. [PubMed: 23376058]
42. Lohmiller JJ, Swing SP, Valli VE, Li X. Epidermotropic Lymphoma (Mycosis Fungoides) in an ICR Mouse. Contemp Top Lab Anim Sci. 1999; 38:47–9. [PubMed: 12086417]
43. Wu X, Sells RE, Hwang ST. Upregulation of inflammatory cytokines and oncogenic signal pathways preceding tumor formation in a murine model of T-cell lymphoma in skin. J Invest Dermatol. 2011; 131:1727–34. [PubMed: 21490619]
44. Rabenhorst A, Schlaak M, Heukamp LC, Forster A, Theurich S, von Bergwelt-Baildon M, et al. Mast cells play a protumorigenic role in primary cutaneous lymphoma. Blood. 2012; 120:2042–54. [PubMed: 22837530]
45. Bassiri H, Das R, Guan P, Barrett DM, Brennan PJ, Banerjee PP, et al. iNKT cell cytotoxic responses control T-lymphoma growth in vitro and in vivo. Cancer Immunol Res. 2014; 2:59–69. [PubMed: 24563871]
46. Ahn JO, Chae JS, Coh YR, Jung WS, Lee HW, Shin IS, et al. Human adipose tissue-derived mesenchymal stem cells inhibit T-cell lymphoma growth in vitro and in vivo. Anticancer Res. 2014; 34:4839–47. [PubMed: 25202065]
47. Demoulin JB, Maisin D, Renauld JC. Ly-6A/E induction by interleukin-6 and interleukin-9 in T cells. Eur Cytokine Netw. 1999; 10:49–56. [PubMed: 10210773]
48. Orabona C, Dumoutier L, Renauld JC. Interleukin-9 induces 24P3 lipocalin gene expression in murine T cell lymphomas. Eur Cytokine Netw. 2001; 12:154–61. [PubMed: 11282560]

Europe PMC Funders Author Manuscripts

Europe PMC Funders Author Manuscripts

Translational Relevance

Current therapies for CTCL are focused on direct targeting of neoplastic cells. However, there is emerging evidence that inflammatory microenvironment plays a pivotal role in the onset and progression of mycosis fungoides. In this study, we demonstrate that IL9 is overexpressed in lesional skin in mycosis fungoides by malignant cells and polarized reactive T cells, suggesting that this cytokine is an active mediator of tumor microenvironment and contributes to the survival of neoplastic cells. Mycosis fungoides patients in remission upon photo(chemo)therapy had lower numbers of IL9-producing cells in the skin, diminished expression of STAT3/5a, and the Th9 transcription factor IRF4. *In vitro* data indicate that IL9 is regulated by STAT3/5 and *in vivo* results highlight the pro-neoplastic effect of IL9 on lymphoma T cells. We propose that targeting IL9, either directly or via STAT inhibition, would be promising for therapeutic intervention in CTCL.

Europe PMC Funders Author Manuscripts

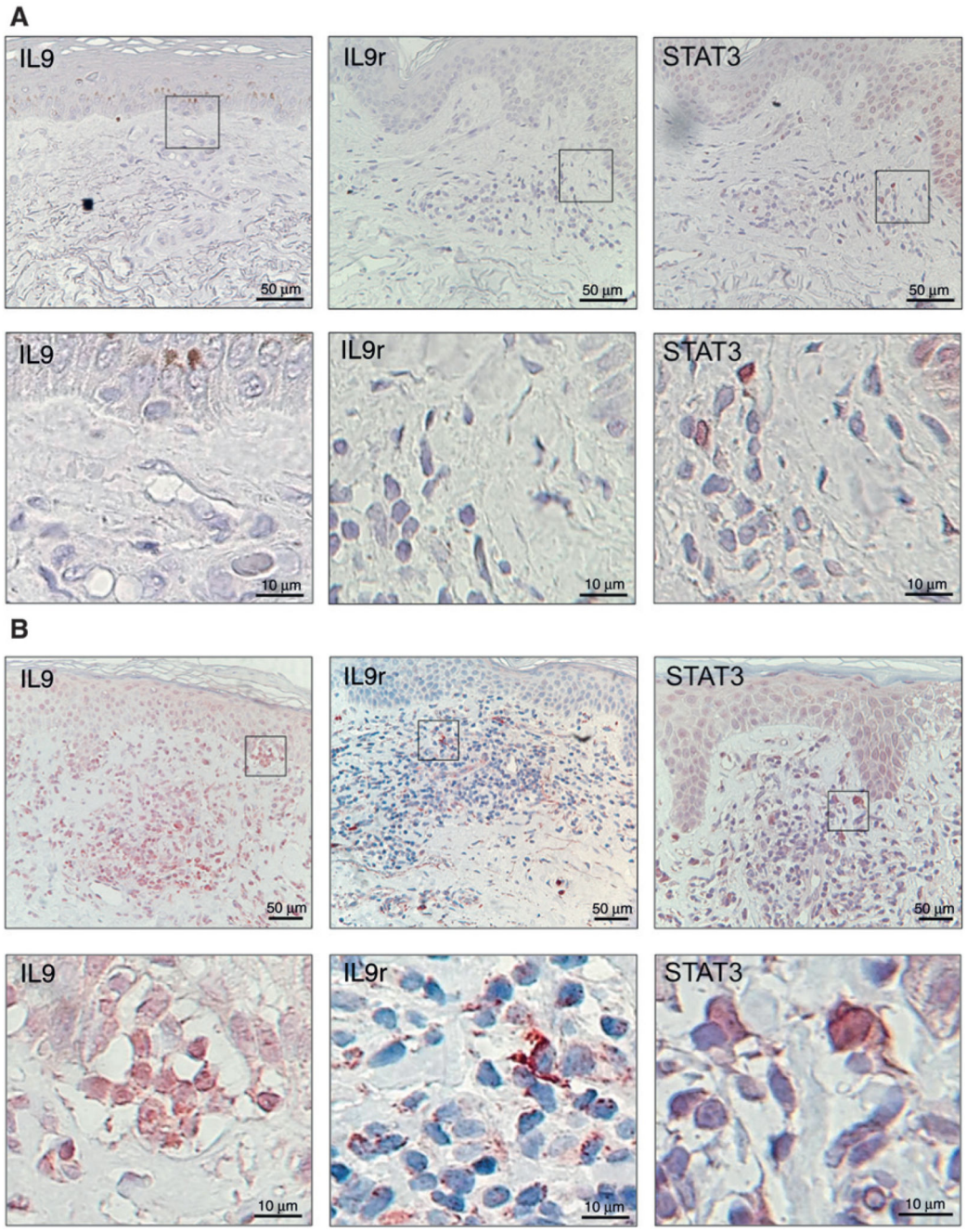

Figure 1.

Expression of IL9, IL9r, and STAT3 in patients with MF. Paraffin-embedded sections were stained for IL9, IL9r, or STAT3. Representative micrographs are shown; magnified areas are indicated. A, normal skin samples from control individuals. B, lesional skin from a patient with MF (archived materials ST2, patient A2), view of 20× (scale bars as indicated). Pautrier microabscess is shown in the magnified area of the IL9 stain.

Europe PMC Funders Author Manuscripts

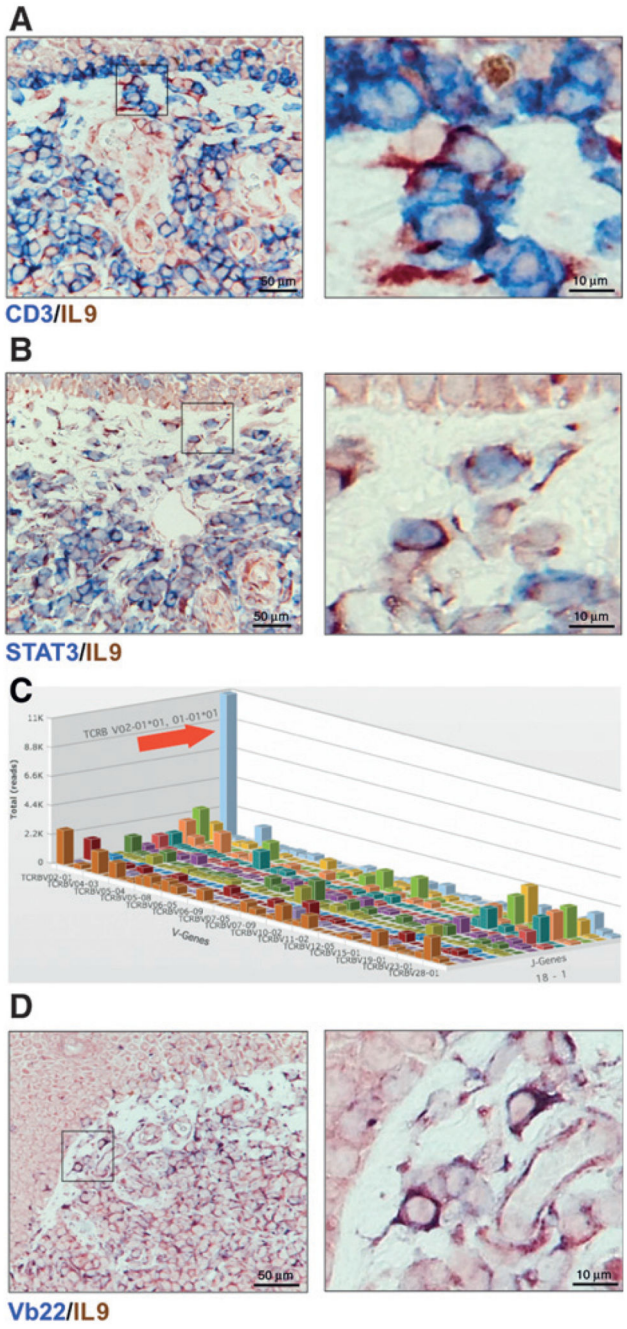

Figure 2.

Malignant and reactive T cells produce IL9. Representative micrographs of two-color IHC (blue/red) in lesional skin of MF patient (ST2, Patient A4) CD3/IL9 (A) and STAT3/IL9 (B); magnified areas are indicated (detailed scoring of double stains are shown in ST2). C, average copy number by V-J pairing of TCRβ sequences by high-throughput sequencing of the CDR3 region (outstanding clone is indicated with red arrow). Immunohistochemical stain of the malignant clone based on sequencing results. The Vb22 antibody was used to identify the TCRβV02-01 gene product (D).

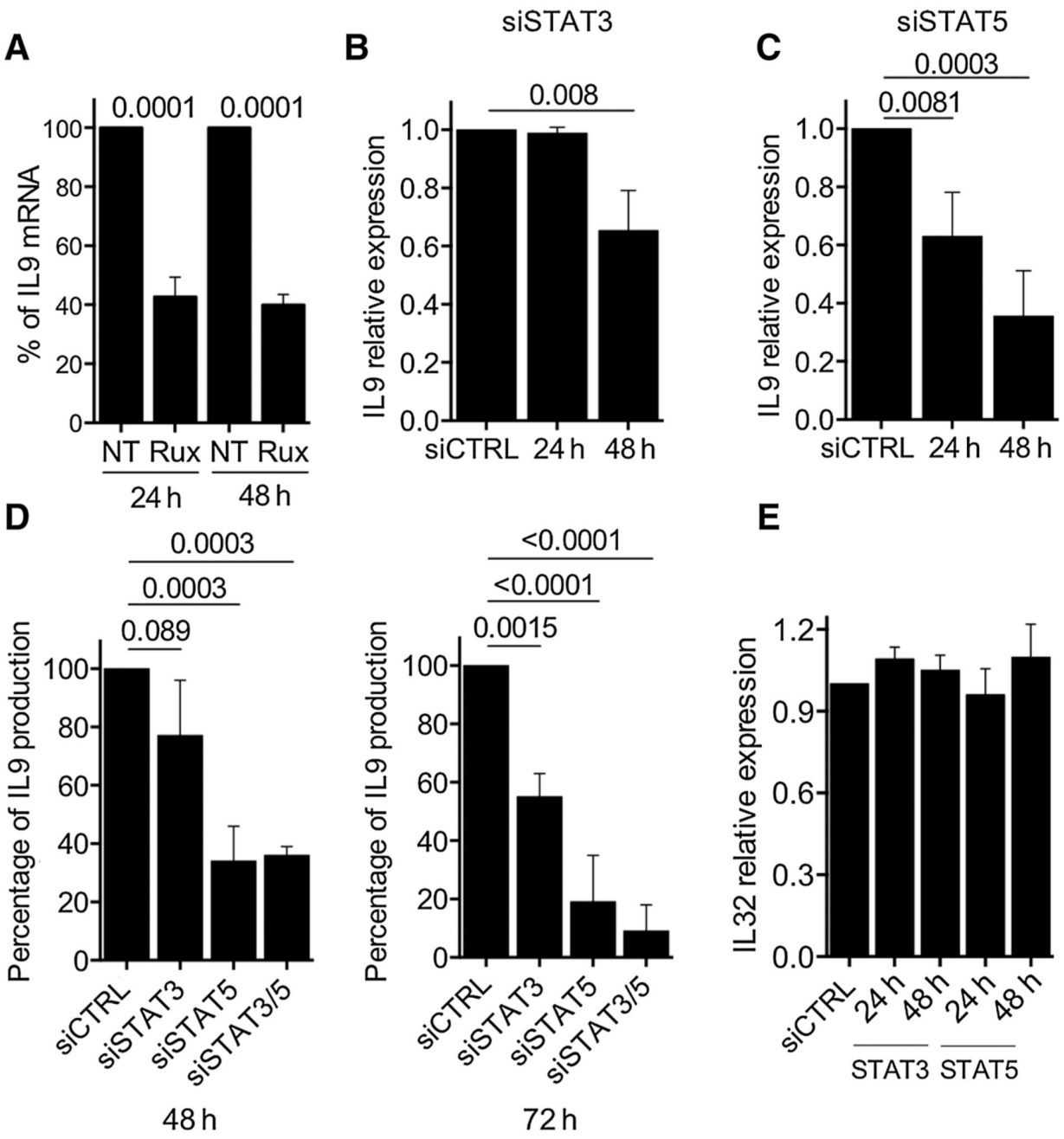

Figure 3.

STAT3/STAT5 pathway regulates IL9 production in MyLa2000 cells. A, MyLa2000 cells were treated with 180nmol/L of ruxolitinib and cultured for up to 48 hours. IL9 expression was quantified by qPCR at indicated time points; not treated (NT) cells were used as controls. MyLa2000 cells were transfected with siRNA targeting STAT3 (B) and STAT5 (C). IL9 expression was quantified by qPCR at indicated time points; fold change is depicted with unspecific siRNA-treated cells (siCTRL) as reference control. D, simultaneous STAT3 and STAT5 silencing. IL9 expression was quantified by ELISA at 48 and 72 hours; siCTRL

cells were used as reference control. E, IL32 expression was quantified by qPCR as control to examine the specificity of the silencing effect on IL9 expression. Experiments were done in triplicates: statistical significance was assessed by Dunnet post test; *P* values are shown.

Europe PMC Funders Author Manuscripts

Europe PMC Funders Author Manuscripts

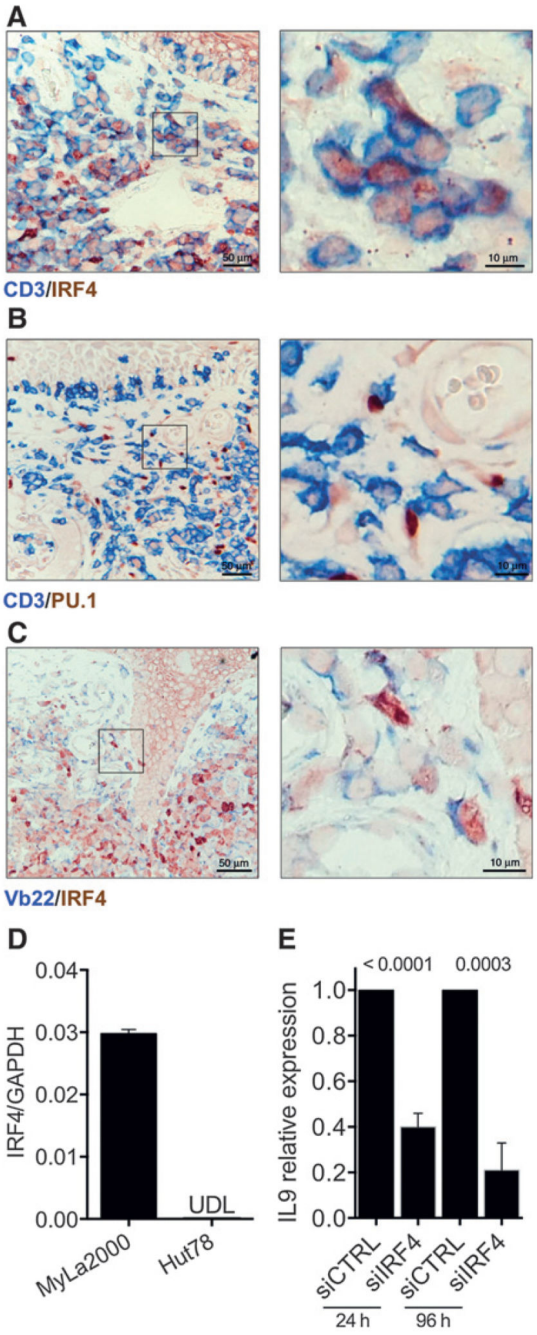

Figure 4.

IRF4 and PU.1 expression in patients with MF. Representative micrographs of two-color IHC are shown. The transcription factors IRF4 (A) or PU.1 (B) were stained together with CD3; magnified areas are indicated (detailed scoring of double stains are shown in ST2). C, malignant cells stained with the Vb22 antibody together with IRF4 (Patient A4 is shown in A–C.). Expression of IRF4 in MyLa2000 and Hut78 cells quantified by qPCR (D) and siRNA was used to silence IRF4. IL9 expression was determined after 24 and for up to 96

hours of transfection (E). Experiments were done in triplicates; statistical significance was assessed by Student unpaired *t* test; *P* values are shown.

Europe PMC Funders Author Manuscripts

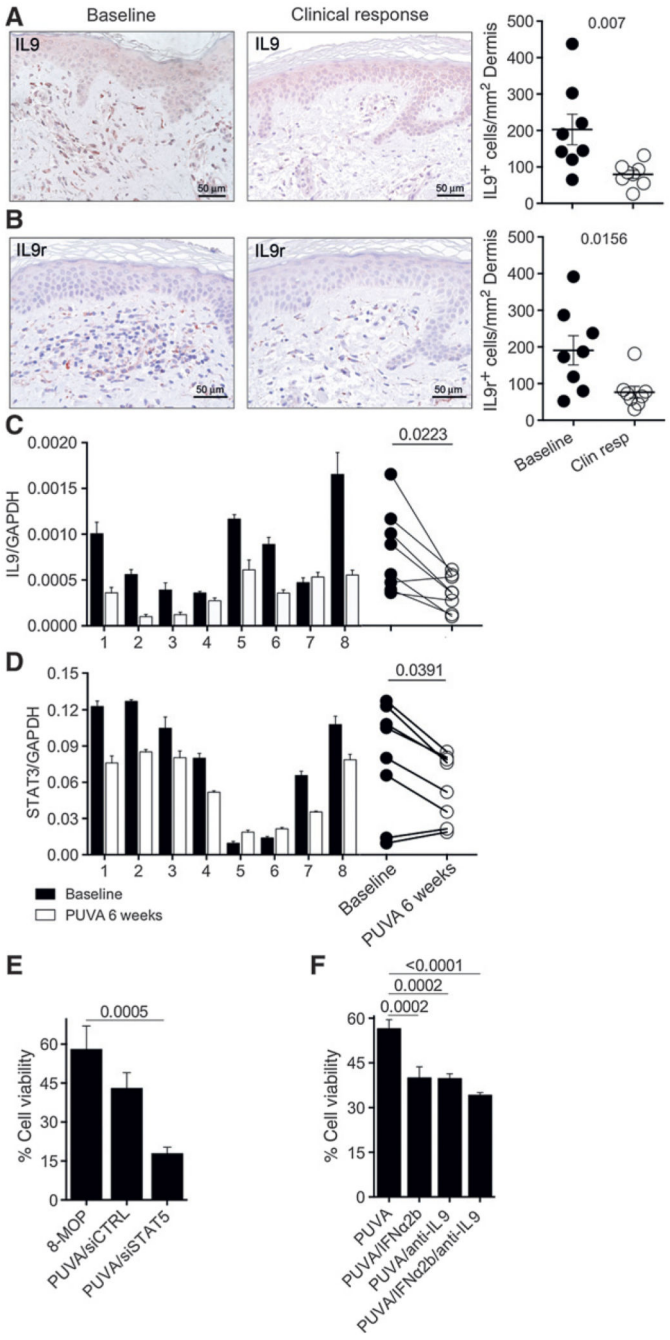

Figure 5.

Patients under photo(chemo)therapy treatment exhibit reduced IL9 production. Samples from the archived materials from patients with MF (ST2) were analyzed for IL9 (A) and IL9r (B) expression at baseline and after 12 weeks at clinical remission (micrographs from patient A1 are shown). The average of positive cells in three 40× fields per sample is presented: adjusted to the unit of area (mm^2). Biopsies from the PUVA trial (ST3) were analyzed by qPCR for expression of IL9 (C) and STAT3 (D) at baseline and 6 weeks after start of treatment. E, MyLa2000 cells were transfected with siSTAT5 or siCTRL 24 hours

before treated with PUVA *in vitro* (1 μmol/L 8-MOP, 0.4 J/cm^2). F, MyLa2000 cells were given PUVA followed by incubation in media supplemented with IFNα2b (1,500 U/mL), goat polyclonal anti-human IL9 antibody (20 μg/mL) or the two combined. E and F, viability was assessed by Annexin V/PI incorporation after 48 hours of culture. Experiments were done in triplicates; statistical significance was assessed by Student paired *t* test (A–D), or Dunnet post test (E and F); *P* values are shown.

Europe PMC Funders Author Manuscripts

Europe PMC Funders Author Manuscripts

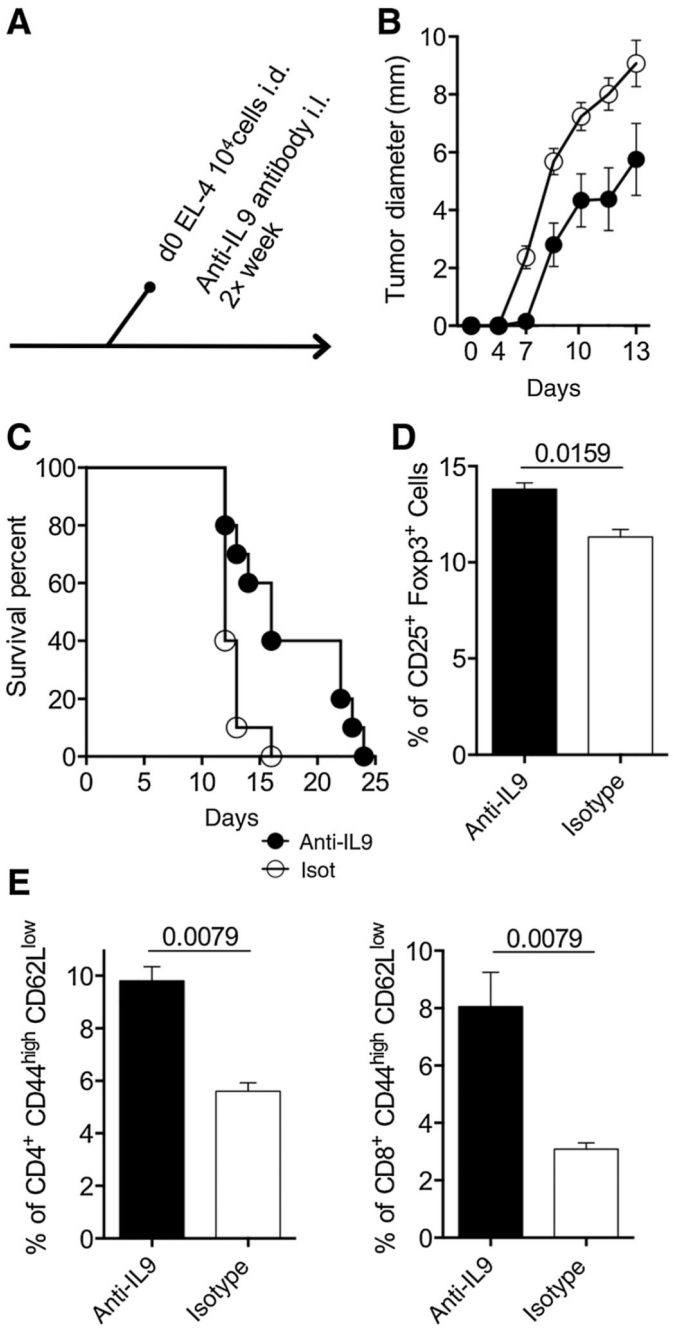

Figure 6.

Depletion of IL9 improves antitumor immune response. Mouse T-cell lymphoma cell line EL4 (10^4 cells) were injected intradermally into the backs of C57BL/6 mice. Polyclonal goat anti-IL9 antibodies (20 μg) or isotype control was given together with the cells and repeatedly every 48 hours (n = 10 mice per experimental group; A). Tumor growth was assessed daily for 14 days using a Mitutoyo Mini-caliper and tumor diameter mean is depicted (B). Mice were sacrificed when tumor size reached 1 cm of diameter; survival is shown (C). Mice were sacrificed 14 days after cell injections and inguinal lymph nodes were

taken to analyze Treg cells by flow cytometry (D) and activated CD4 and CD8 T cells (E; n = 6 mice per experimental group). The percentage of positive cells is presented. Figures shown are representative of two independent experiments. Statistical significance was assessed by Student t test; P values are shown.

Europe PMC Funders Author Manuscripts